СВЕСКЕ ФИЗИЧКИХ НАУКА
SFIN year XIV Series A: Conferences No. A1 (2001)

20th SPIG

THE PHYSICS OF IONIZED GASES

**INVITED LECTURES,
TOPICAL INVITED LECTURES AND PROGRESS REPORTS**

Editors:
N. Konjević, Z. Lj. Petrović, and G. Malović

**Institute of Physics
Faculty of Physics, University of Belgrade
Institute of Nuclear Sciencies "Vinča"
Belgrade, Yugoslavia**

YU ISSN 0354-9291
YU ISBN 86-82441-08-X

THE PHYSICS OF IONIZED GASES
SFIN year XIV No. A1 (2001)

20th Summer School and International
Symposium on the Physics of Ionized Gases

20th SPIG

September 4. – September 8. 2000, Zlatibor, Yugoslavia

THE PHYSICS OF IONIZED GASES

INVITED LECTURES,
TOPICAL INVITED LECTURES AND PROGRESS REPORTS

Dedicated to the memory of prof. Milan Kurepa

Editors:
N. Konjević, Z. Lj. Petrović and G. Malović

Institute of Physics,
Zemun, Yugoslavia

Faculty of Physics, University of Belgrade,
Belgrade, Yugoslavia

Institute of Nuclear Sciences "Vinča",
Belgrade, Yugoslavia

СВЕСКЕ ФИЗИЧКИХ НАУКА
SFIN year XIV Series A: Conferences No. A1 (2001)

THE PHYSICS OF IONIZED GASES

Edited by
N. Konjević
Z.Lj. Petrović
G. Malović

SPIG 2000

SFIN, XIV (A1), 1 -531, Belgrade 2001

Institute of Physics, Belgrade, Yugoslavia

СВЕСКЕ ФИЗИЧКИХ НАУКА

UDK 53

Series A: Conferences

SFIN, year XIV, No.A1 (2001)
YU ISSN 0354-9291

Publisher
Institute of Physics, Belgrade

Editorial Office
S F I N
Institute of Physics
P.O.Box 57
Pregrevica 118, Zemun
11001 Belgrade, Yugoslavia

Ministry of Science, Technology and Development of the Republic of Serbia supports the publication of this journal

---

The price for this issue is din. 800.00 (foreign $50.00). Students are qualified for reduced rates. Please place your orders and inquiries to "BF Club", P.O.Box 86, 11080 Zemun, Yugoslavia, fax + (381) 11 186-105.

Printed by:
Public Enterprise of PTT Traffic "Srbija"
Publishing Department, Belgrade – Yugoslavia

Number of copies: 220

20th SPIG

SCIENTIFIC COMMITTEE

N. Konjević, Chairman, Yu

N. Bibić	YU	K. Lieb	GER
S. Buckman	AUS	T. Makabe	JPN
M. Dimitrijević	YU	B. Marinković	YU
S. Đurović	YU	N. Nedeljković	YU
T. Grozdanov	YU	Z. Petrović	YU
D. Jovanović	YU	M. Radović	YU
M. Kono	JPN	M. Škorić	YU

ORGANIZING COMMITTEE

Z. Petrović, Co-Chairman
N. Bibić, Co-Chairman
M. Kuraica, Co-Chairman
G. Malović, Secretary
Lj. Hadžijevski
N. Kos
N. Šišović
B. Marinković
M. Radetić
A. Strinić
Z. Raspopović
D. Marić
N. Sakan

CONTENTS

Section 1. ATOMIC COLLISION PROCESSES

Section 2. PARTICLE AND LASER BEAM INTERACTION WITH SOLIDS

INVITED LECTURES

PROGRESS REPORTS

Section 3. LOW TEMPERATURE PLASMAS

INVITED LECTURES

COMPLETING OF ELECTRON-ATOM SCATTERING PICTURE FOR ARGON AND THE RARE GASES

D.M.Filipović* and B.P.Marinković[+]

**Faculty of Physics, University of Belgrade, PO Box 368, 11001 Belgrade, Yugoslavia*
[+]Institute of Physics, PO Box 57, 11001 Belgrade, Yugoslavia

Abstract. Electron-atom scattering picture is not complete, even for unpolarised incident electrons and argon, almost a century after the Lenard's pioneering works. Such criticism particularly has weight in the case of Ne, Kr, Xe and Rn.

A great deal of effort was devoted to measure differential and integrated cross sections for both elastic and inelastic scattering of electrons by Ar and the rare gases, except Rn. Performances of apparata used in such kind of experiments are in permanent progress. Separation of inelastically scattered electrons from elastically scattered is the solved problem, even at the primary beam direction. But, the back-scattering is attained recently, by using a sophisticated technique. As jet, electron optics is of inferior resolution with respect to light optics; only lower excited states of argon and the rare gases are resolved in the electron energy-loss spectra.

From the measurements we can obtain many information about processes that are not too complicated, like elastic scattering. It is easy to visualize such process and to estimate: (a) relative contribution of effects of long-range Coulomb and short-range exchange interactions to the cross sections, (b) position of critical points – where differential cross section attains its smallest values and (c) relative atomic diameter. For processes that are more complex, measurements were generally carried out only at a few impact energies. So, it is not easy to estimate the effects of: electron "absorption", statistical weight ratios of the fine structure states, scattering at small angles etc.

A more thorough knowledge about a structure (rapid decrease) in the elastic integral cross sections for Ar and Xe at intermediate energies (10-100 eV) required a new approach and more precise measurements.

1. INTRODUCTION

Nineteen seven years ago, Lenard[1] published an experiment of electron - gas atom collisions with the aim to throw more light to both the constituents and the structure of matter. Results of that experiment with argon (and a few molecules) as a target, attracted a great interest, especially as a base for a model of the atom, well known at the present as the Lenard's model. A decade after, observation of a substantial energy absorption in inelastic electron-atom collisions, by Franck and Hertz[2], was an elegant proof of Bohr's theory of the hydrogen atom. Both experiments pointed out lower incident electron velocities, at which the collision involves a number of complex processes, as more convenient to perform new fundamental experiments.

It is thorough why Ramsauer[3] designed an apparatus in which incident electrons were accelerated by the electric field and selected by the magnetic field to well defined low velocities. In this way, result of extraordinary decreasing of the effective cross section for scattering of slow incident electrons by argon, obtained previously by Mayer[4], was confirmed. Ramsauer extended the measurements to He, Ne, Kr and Xe, and found the same effect in the case of Kr and Xe. Theoretical description of this effect by Faxen and Holtsmark[5] was based on Rayleigh's ideas related to a sound wave as a sum of its harmonics. The elastic cross section of an atom has presented as the sum of the partial cross sections over all partial waves (i.e. angular momentum quantum numbers) of the incident wave. Bohr suggested the explanation for the falling down of the cross section: Spherical potential of Ar, as well as of Kr and Xe, may be deep enough to introduce one or more complete wavelengths of zero angular momentum, so the scattering can not been observed far from the atom.

Arnot[6] designed an apparatus for the angular distribution measurements, searching for new information about electron-atom scattering. He found remarkable decrease of intensity for electrons elastically scattered by argon at scattering angles from 0° to 60°. After a few months, Bullard and Massey[7] realized the same experiment, but using their apparatus with the angular region extended to 125°. They found local minima and maxima of the angular distribution curves and explained them by the electron diffraction. It was the first experimental proof of a wave nature of the electron in binary electron-atom scattering. Wave-mechanical treatment of the scattering has been formulated by Born[8]. He generalized the Huygens-Fresnel principle to electron-atom scattering and introduced a reasonable approximation. The complete theory must include effects assigned by Mott and Massey[9], as:

scattering of electrons by a static atomic field, exchange of incident and atomic electrons, distortion of the incident wave, distortion of the atomic field due to electric polarization (and/or excitation) and interaction between elastic and inelastic channels.

New information were found by studying structures in total and integrated cross sections. Schulz[10] found a resonance structure in electron-helium total cross section. Orbiting effect was too simplified classical model for explanation of a temporary negative ion formation, what the resonance actually is. For a shape resonance, wave-mechanical model is adopted, which predicts formation of a barrier in the electron-atom interaction potential and decay of the resonance by the tunneling effect.

Also, coupling between elastic and inelastic channels causes decreasing of the elastic scattering cross section. Mittleman and Watson[11] showed, following Yoshioka's idea,[12] that the effect of inelastic scattering could be a loosing of electron flux for the elastic channel, theoretically represented as an imaginary component of the scattering potential. Joachain and coworkers were successfully applied this model to electron-helium and more complex atoms, but not below 100 eV incident electron energy. Bartschat *et al*[13] used a ten-state optical potential method to improve their polarized-orbital approximation for argon at intermediate energies (15-100 eV).

Estimation of the order of magnitude of the collision time is important in considering of a role of "small" (weak and of little relevance) forces, which induce splitting of atomic levels. Transition between split levels is convenient to describe on a time scale; if the collision time (τ_{coll}) is large compared to the relaxation time τ as a reference, the small forces could play significant role during the collision. In a classical picture, adopted by Bederson[14], $\tau_{coll} = L/v$, where L is the effective linear dimension of the atom, and v is the velocity of the incident electron. Percival and Seaton[15] involved the "complete passage time of the wave packet", as a more complete description of duration of an electron-atom collision. The uncertainty principle of Quantum physics (in the form: $\Delta t \approx \hbar/\Delta E$) is not correct to use for this purpose, because it represents the uncertainty in time when the collision occurs, not the duration of the collision. It has no satisfactory relation jet for the duration of electron-atom collision.

In this lecture, a lot of details on elastic electron scattering by argon and the rare gases are given at intermediate energy region. Differential cross sections (DCS) and integral cross sections (Q_i),

$$Q_i(E) = 2\pi \int_0^{\pi} DCS(E,\theta)\sin\theta d\theta, \qquad (1.1)$$

where E is the incident electron energy and θ is the scattering angle, are quantities which enable consideration the effects of fundamental processes in order to understand the nature of the electron and the target atom in the collision. We will use the effective atomic diameter d_{eff}, via geometrical interpretation of $Q_i(E)$, beside the $Q_i(E)$ itself.

Typical experimental techniques are described in Section 2. Experimental results for Ar and the rare gases are presented in Section 3. The experimental and theoretical results are discussed in section 4. Finally, the list of references is given.

2. THE EXPERIMENTS

Electron spectroscopy is well-established experimental method for analyzing electron-atom interactions in binary collisions. A lot of measurements of electron collisions with atoms in gas phase have been performed up to now. Advances in improving the possibilities of this method have been concentrated to parts of the experimental apparatus: electron sources, optical lenses, energy selectors and detectors. In the field of electron detection, single electron counting technique is normally used. The modern experiment enables to resolve elementary processes - such that initial and final states are separate stationary states of atoms. In this lecture we are interested only in unpolarized incident and scattered electrons, and atomic states well-defined by clearly separated peaks in energy-loss spectra (see 2.2.2).

2.1. Old experiment

As example of old experiments of electron – gas atom collisions can serve the Lenard's apparatus and procedure, mentioned in the Introduction. Lenard designed an apparatus for measurement of the absorption of "cathode-rays" in gases. He prepared incident electrons of extremely low velocities with respect to that from β-decay of Ra, previously used. The apparatus is presented schematically in figure 2.1.

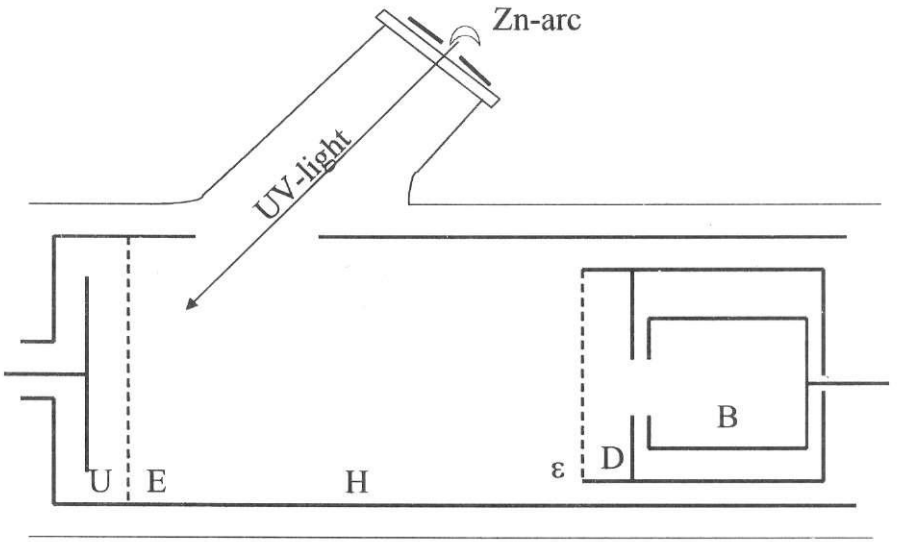

Figure 2.1. Scheme of the Lenard's apparatus.

The electrode U is the source of electrons when is illuminated by UV radiation from a Zn-arc lamp. Metallic envelope H, wire gratings E and ε and aperture D are at referent (earth) potential. The Faraday cup B, connected with a sensitive quadrant electrometer, is employed as a detector. Subsystem εDB is movable in H, so the path of the electrons through the gas is $d = UD \approx E\varepsilon$. The velocity of incident electrons is controlled by the negative potential of the electrode U. All the elements H, U, E, D and B, were of the same contact potential, except ε which was made of platinum.

The tube was evacuated before involving of the sample gas. Carefully measured working gas pressure was of the order of (0.1 – 1) Pa.

If the tube is evacuated, the indication of galvanometer is proportional to the current

$$J = Ae^{-\alpha' d}, \qquad (2.1.)$$

where α' is the "absorption power" of a residual gas and A is a constant. If the tube is filled with a sample gas, the indication of the galvanometer decreases due to scattering of the electrons by atoms in the interaction volume and corresponds to the current

$$i = Ae^{-(\alpha+\alpha')d}, \qquad (2.2.)$$

where α is the absorption power of the sample gas.

From equations (2.1) and (2.2) Lenard derived a formulae for determination of α, according to the quantities measured in the experiment

$$\alpha = \frac{1}{d}\ln\frac{J}{i}. \qquad (2.3)$$

Rather than α, Lenard established the "specific absorption power", $\alpha_0 = \alpha/p$, where p is the sample gas pressure. According to observations on slow electron beams in the air and hydrogen molecules, he assumed α_0 is a fundamental quantity at a certain temperature. Definitely, experimental results for the gases were normalized to the result on aluminum at high velocity and presented graphically in the form $\sqrt{\alpha_0}$ vs. velocity (in units of $\sqrt{V}$).

2.2. Modern experiment

We will describe the electron spectrometer built in our laboratory, as an example of modern apparatus. New results that can be achieved by using of polarized electron spectroscopy as a fundamental technique extend the meaning of the elementary processes adopted above.

2.2.1. Monochromator

Electrons are obtained from a hot filament with energy distribution from zero to approximately 0.4 eV. Accelerating potentials of a few hundred volts maximize the flux of extracted electrons. Then, decelerating potentials prepare the electrons for energy selection at the energy of a few eV. Windows and pupils collimate the electron beam; deflectors take the beam to draw along the optical axis. Hemispherical electrostatic energy selector is a dispersion element of the electron optics. Only a narrow band of the energy distribution transmits with it. A compromise between a high flux and a narrow energy distribution is always present. After the energy selector, the electrons are accelerated to a desirable energy

and focused to a center of interaction. Windows and pupils collimate the beam and deflectors diminish its deflection with respect to optical axis. The term *monochromator* is adopted for electron-optical systems such as just described, due to strong analogy between light and electron optics.

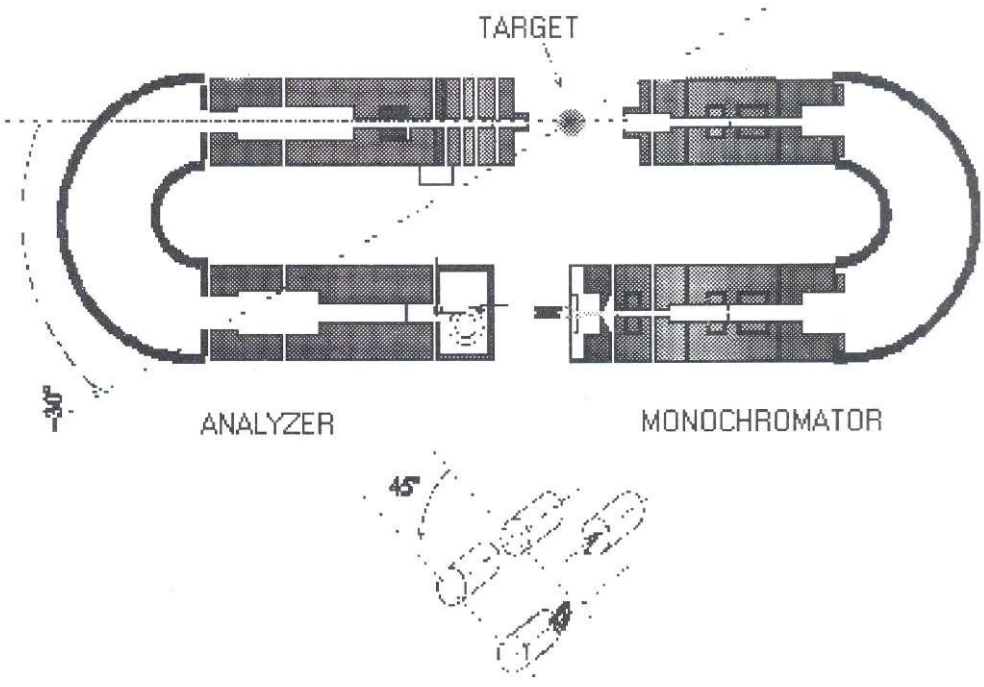

Figure 2.2. Scheme of the electron optics of the electron spectrometer.

2.2.2. Analyzer

The analyzer is performed to accept scattered electrons of residual energies down to a few eV, in the angular range from -30° and 150°. Electron optics of the analyzer, similar to that of the monochromator, is tuned to transmit only elastically scattered electrons. If the addition of energy to the inelastically scattered electrons is equal to the energy loss of incident electrons in a particular scattering process, such electrons will pass through the analyzer and will be detected. The channel electron multiplier in a single-electron-counting mode is employed as a detector. A spectrum of intensity of scattered electrons obtained by changing the accelerating potential is an energy-loss spectrum. Each peak in this spectrum corresponds to a level of excitation of a given target atom.

2.2.3. Collision chamber

Both the monochromator and the analyzer are in the separate part of the metallic collision chamber, differentially evacuated to ~10^{-5} Pa. The interaction volume is identified by the incident electron beam and the atomic beam, which are mutually crossed at a right angle. Pressures of the order of 1 Pa or less are required to avoid multiple scattering[16]. In narrow beam geometry, the angular resolution is given by an acceptance angle rather than by a view angle of the analyzer. The overall energy resolution is a sum of two parts. The first is that of monochromator as a FWHM (full width at a half maximum) of the incident electron energy distribution at interaction volume, and the second is of analyzer. The second part contributes with 1/3 to the overall resolution due to lower technical complexity and a lower filling factor of the electron lenses. Elements of electron optics (primarily hemispherical energy selectors) are bakeable in a high vacuum to remove insulating films. Also, double μ-metal shield reduces a stray magnetic field to 10^{-7} T or less. So, stray electrostatic and magnetic fields, which distort the trajectories of the electrons, are avoided.

Performances of this spectrometer are good enough to resolve peaks in energy-loss spectra obtained by excitation of lower stationary states of argon and the rare gases.

The scattering signal is proportional to the cross section. According to Brinkmann and Trajmar[52], the scattering intensity is

$$I(E,\Delta E,\Omega)=\int_{\vec{r}}\int_{E'}\int_{\Delta E'}\int_{\Omega'(\vec{r})}\rho(\vec{r})f(E',\vec{r})F(E',\Delta E',\Omega'(\vec{r}))DCS'dE'd(\Delta E)'\partial\Omega'(\vec{r})d\vec{r}\,, \qquad (2.4)$$

where: E is the nominal incident electron energy, ΔE – nominal energy loss and Ω(θ,φ) –nominal scattering angle, $\rho(\vec{r})$ -density distribution of target atoms, $f(E',\vec{r})$-combined distribution of incident electrons, F is geometrical factor, and DCS' is the triple differential cross section for a certain process. Rather than absolute, we performed relative DCS measurements. Normalized absolute DCS values were obtained applying the most reliable cross sections available in literature.

2.3. Apparatus for demonstration of the Ramsauer-Townsend effect in a simplified way

It is easy to involve electron-atom collision experiments in every student's atomic physics laboratory. For example, Kukolich[17] devised a simplified way to demonstrate the Ramsauer-Townsend effect in Xe, using a 2D21-thyratron. Electrode structure of the tube (see figure 2.3) is suitable for an electron transmission technique.

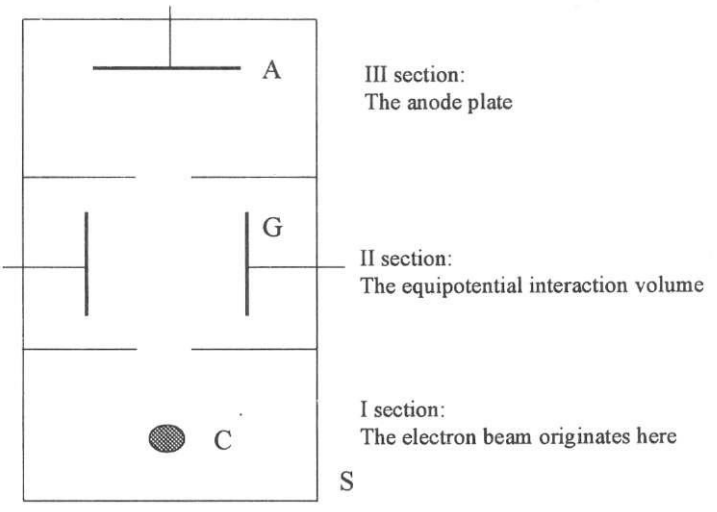

Figure 2.3. Scheme of the electrode structure of 2D21 thyratron.

The cathode C is operated on ~2 V DC instead of 6.3 V, so space charge effects are diminished. Electrons from the C pass through an equipotential interaction region defined by the grid G and two apertures where the scattering by the Xe atoms takes place. The equation

$$I_A = I_S F(1 - P_S) \qquad (2.5)$$

gives the anode current I_A as a function of the shield current I_S, geometrical factor F ($I_S F$ is the anode current if the interaction region is empty) and P_S is the probability of scattering. To determine F, the Xe is freezing out taking the tube in liquid nitrogen, at 77 K. P_S falls down, so if we assign quantities obtained at this temperature with asterisks, the equation

$$F = \frac{I_A^*}{I_S^*} \qquad (2.6)$$

is valid in a good approximation. Involving equation (2.6) into equation (2.5), the probability of scattering is given by the measurable quantities, as

$$P_S = 1 - \frac{I_S}{I_A}\frac{I_A^*}{I_S^*}. \qquad (2.7)$$

This demonstration has been successfully using in our student's laboratory. In addition, the phase sensitive detection (PSD) technique[18] is realized, as an extension of the original Kukolich's design. In this way, some structures are obtained at energies above the cross section maximum, existing in results of sophisticated experiments[19,20] and in recommended values.[21]

3. EXPERIMENTAL RESULTS

Argon and the rare gases: He, Ne, Kr and Xe, were the first atoms that are experimentally investigated for binary electron-atom collisions. Differential cross section curves are analogous to diffraction pattern of the light. As an illustration, the observed elastic DCS's for incident electrons of 20 eV energy are shown in fig 3.1.

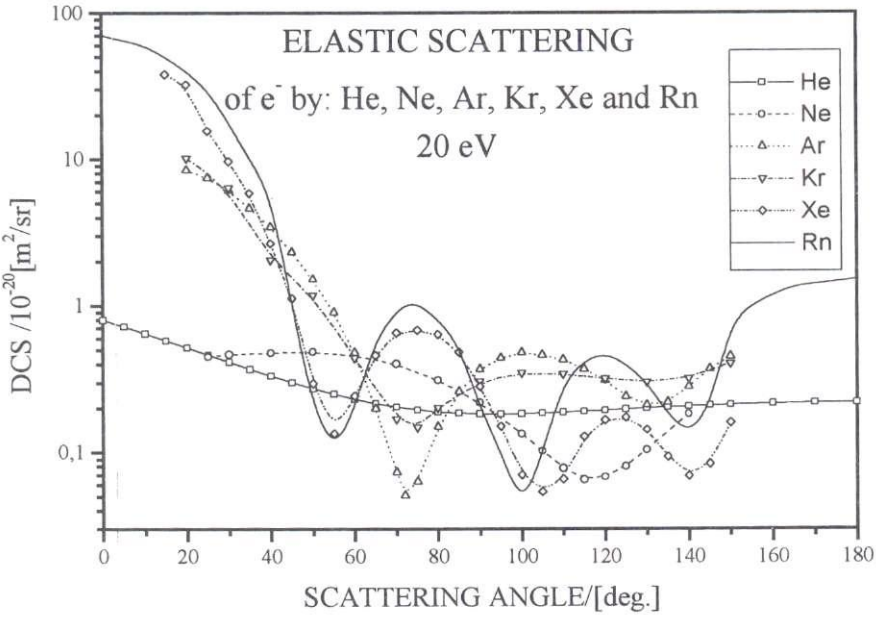

Figure 3.1. Differential cross sections for: He[22], Ne[23], Ar[24], Kr[25], Xe[26] (experiments) and Rn[27] (calculation), at 20 eV incident electron energy.

The total cross sections (Q_t) for Ar, Kr and Xe atoms are of fundamental interest because their rapid decrease and deep minimum at low incident electron energy (<1 eV) is well known Ramsauer-Townsend minimum. There is not such structure in the case of He and Ne.

3.1. Argon

Argon is a constituent of the earth's atmosphere in amount of almost 1%, so it is not rare. But, it is a "noble" or "inert" as well as the rare gases: He, Ne, Kr, Xe and Rn (which is radioactive).[28]

We have used argon as a probe gas in the electron spectrometer mentioned above (§ 2.2), so several e/Ar collision processes have been repeated many times. The results of elastic DCS measurements were analyzed to obtain DCS minima positions and the critical minima.[24] Using simple Fraunhofer formulae one can search an n-order DCS minimum position

$$\theta_{min} = \arcsin(n / D_\lambda) \qquad (3.1)$$

where $D_\lambda = d_{eff}/\lambda$, is the reduced effective atomic diameter. Because de Broglie wavelength of an incident electron, λ, and corresponding effective atomic diameter, d_{eff}, depend of collision energy on a different power, D_λ is a function of the energy as well. Recently, we published our results of electron-impact excitation of the lowest four 4s- and also two 4p- states,[29,30] so we recommend these papers as a support to this lecture.

3.1.1. Total cross section

Experimentally, argon is a favorite because their relatively large cross sections for electron collision processes, with respect to He and Ne, make a picture about argon as a large atom. If the length scale is the de Broglie wavelength of the incident electron, $D_\lambda \sim 1$ for argon in the energy region from 10 to 100 eV. Comparisons of total cross sections for argon are presented in figure 3.2.

Here, we will not compare sum of our $Q_i + Q_{exc}$ (elastic integral + total excitation) cross sections at certain energy and corresponding ionization cross section (Q_{ion}), with total cross sections presented in the figure. Rather, we used the total cross section of Jost *et al*[20]

and the total ionization cross section of Straub *at al*[37] to re-normalize our both elastic and excitation cross sections, in a following way.

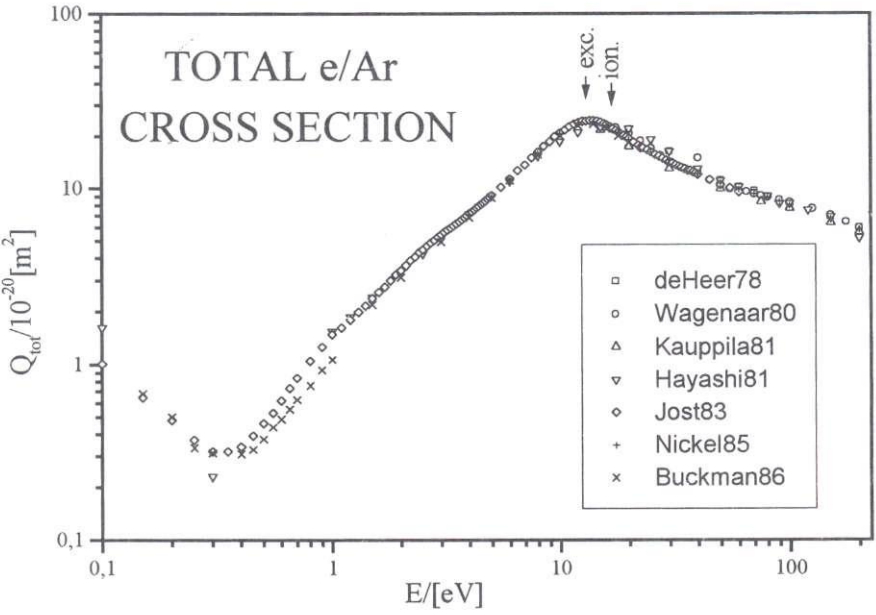

Figure 3.2. Experimental total cross sections for electron-argon collision: □, de Heer *et al*[31] (semi – empirical); ○, Wagenaar and de Heer[32]; Δ, Kauppila *et al*[33]; ∇, Hayashi (recommended)[34]; ◊, Jost *et al*[20]; +, Nickel *et al*[35]; ×, Buckman and Lohman[36].

At a certain collision energy, the equation

$$Q_{tot} - Q_{ion} = Q_i + Q_{exc}, \qquad (3.2)$$

and our experimentally determined elastic-to-excitation ratio, Q_i/Q_{exc}, underline our more precise elastic integral cross sections and the effective atomic diameters for elastic scattering process.

3.1.2. Elastic scattering

There are many results of the elastic DCS measurements for argon, but only several authors have sufficient number of the energies between 10 and 100 eV, precise enough to be able to obtain $Q_i = Q_i(E)$ curve. We have measured elastic DCS's for argon at twelve incident

electron energies. Many DCS results are important because we will discuss the structure (rapid decrease of Q_i) which appears in this energy region. Elastic integrated cross sections for argon are re-normalized as it is explained above. In this procedure we utilized our preliminary results of the total excitation cross sections. The result of determination of the reduced effective atomic diameter, $D_\lambda = D_\lambda(E)$ that is the quotient of the effective atomic diameter and the de Broglie wavelength of the incident electron, is presented in figure 3.3, together with the same quantity extracted from available elastic DCS's for argon.

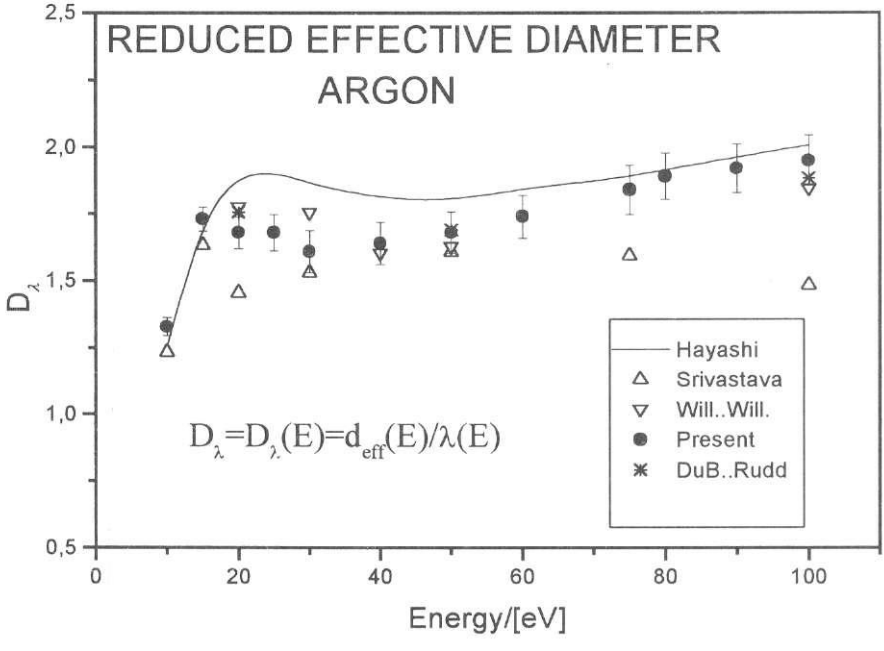

Figure 3.3. Experimental the reduced effective atomic diameter in elastic scattering of electron by argon: —, Hayashi (recommended values)[34]; Δ, Srivastava *et al*[38]; ∇, Williams and Willis[39]; *, DuBois and Rudd[40].

As a result of the re-normalization, the error of D_λ is within 0.1 (or 10%), so it is easier to estimate weather the structure exists or not.

3.2. Helium and Neon

Helium and neon are the atoms for which the Ramsauer-Townsend effect is not observed. Helium is atom that has been extensively studied both experimentally and theoretically. In the experiments it serves for calibration of: (a) impact energy scale which changes due to contact potentials, using the sharp resonance at 19.38 eV[26], (b) transmission of the analyzer using the part of ionization continuum which has a constant value and (c) absolute DCS scale for other gases, by measuring sample gas – helium intensity ratios and applying absolute He DCS's proposed as a standard.[41]

In opposite to shallow DCS minima in He, very deep DCS minimum is observed in Ne at so-called critical point, that is pair of the scattering angle and the energy at which DCS attains it's the smallest value. In searching for a structure at the critical point we analyzed results of e/Ne DCS minima position (figure 3.4).

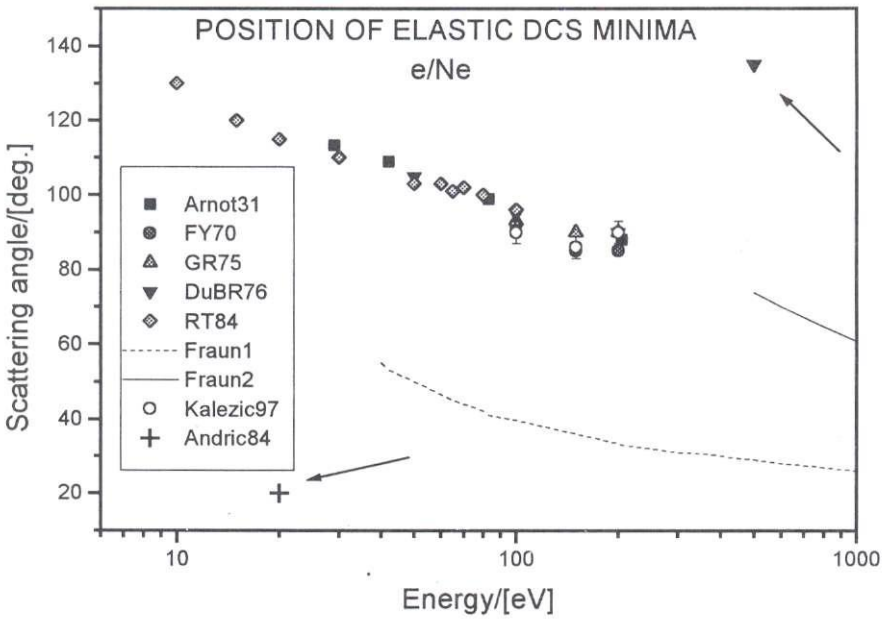

Figure 3.4. DCS minima position in e/Ne elastic scattering: ■, Arnot[43]; •, Fink and Yates[44]; ▲, Gupta and Rees[45]; ▼, Du Bois and Rudd[40]; ♦, Register and S. Trajmar[46]; ○, Kalezić *et al*[42]; +, Andric[47]; -- and —, I and II minimum from the Fraunhofer formula, respectively. Two extreme minima positions are assigned with arrows.

According to available results, a cross section minimum moves to smaller scattering angles as the electron energy is increased. A limit of this trend in vicinity of 150 eV, and the opposite behavior at higher energies, is confirmed with a shallow minimum at 500 eV, found by DuBois and Rudd.[40] Analysis in details shows the "accumulation" of minimum deflection angles around 90° and 150 eV, i.e. far from the critical point experimentally determined by Kollath and Lucas (103° and 73.7 eV)[48]. It seems that the critical point corresponds to a larger angle minimum, which is without prominent structure in vicinity of this point, were a "collapse" of the DCS appears.

3.3. Krypton, Xenon and Radon

Krypton, xenon and radon are the heavy atoms for which relativistic effects in electron scattering are significant. The structure of elastic DCS's is similar to that of Ar. The structure for Xe is more rich and similar to that predicted for Rn. Our analysis of DCS's at the energies from 15 to 80 eV and scattering angles from 20° to 150°, shows the existence of two and four minima for Kr and Xe, respectively. We found two, one and three critical points for Ar[24], Kr and Xe, respectively, in the energy region between 10 and 100 eV. This is in good agreement with results of Kessler *et al*[49].

Resonance structures in elastic electron scattering in the backward hemisphere were observed by Zubek *et al*[49]. In measurements from 105° to 180°, resonance structures in Kr and Xe were observed. These structures correspond to the $^2P_{3/2}$ and $^2P_{1/2}$ negative ion resonances of respective atoms. The energy scale has been calibrated with respect to that of argon $^2P_{3/2}$, also presented in the contribution. New searching for the structures at higher energies (10-100 eV) are desirable from the same (Manchester University) group.

Radon is the heaviest rare gas, existing as a decay product of uranium and thorium. Radon itself decays via polonium, lead, bismuth and thallium isotopes to stable lead. The most interesting of the three naturally occurring radon isotopes is ^{222}Rn, from ^{238}U decay chain. The ^{222}Rn is a direct product of the ^{226}Ra decay. Radon decays, with a half-life of 3.82 days, via polonium, lead, bismuth and thallium isotopes to stable lead. The Rn melting point is of 202 K, boiling point of 211 K and a density of 9.73 kg/m^3 (at normal temperature of 298 K and normal pressure of 1 bar). When is cooled at 77 K (the temperature of liquid nitrogen, conventionally used in physics laboratories) radon exhibits brilliant phosphorescence from yellow to orange-red. Just before a century, Dorn discovered ^{222}Rn, emanating from Ra.[50] Radium β-decay from thick-well glass cylinder was used as a source of fast

"Kathodenstrahlen" by Lenard[1] in study of electron absorption in gases (see § 2.1). A continuous β-ray spectrum from a thin-walled capsule containing radium was used by Randels *et al*[51], in study of the single scattering of electrons in Ar, Kr and Xe gases. Radium was extensively used in atomic physics experiments, and radon isotopes continuously emanated from, but in our best knowledge, there are not results of electron-Rn atom scattering experiments, up to now.

Results of $D_\lambda = D_\lambda(E)$ for Kr, Xe and Rn, in the energy range from 10 to 100 eV, are presented in figure 3.5. Local minimum The error of D_λ is comparable with 0.1 (10%). Comparison with results extracted from Q_i values recommended by Hayashi shows agreement in shape. Local minimum between 10 and 100 eV is clearly visible.

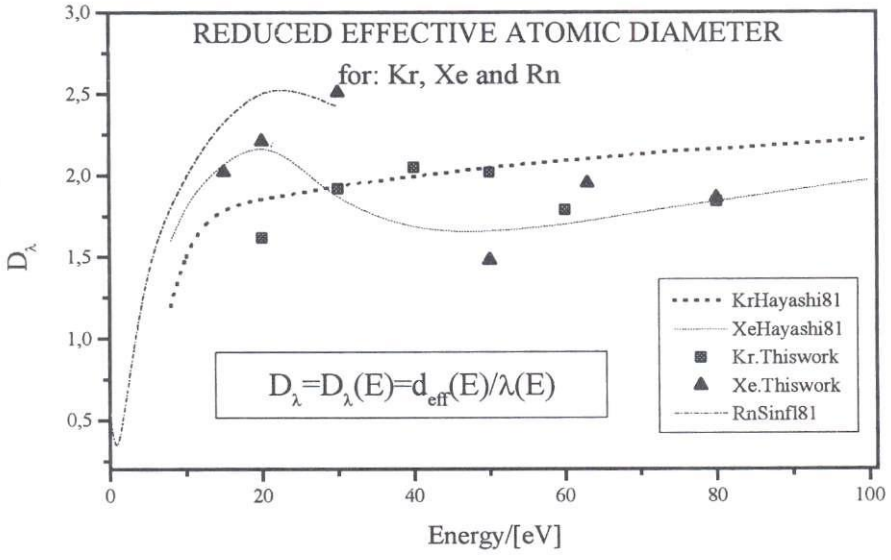

Figure 3.5. Reduced effective atomic diameter in elastic scattering of electron by Kr, Xe and Rn: --- and ···, Hayashi, recommended values for Kr and Xe, respectively[34]; -·-, SinFaiLam[27]; ■, our Kr and ▲, our Xe experimental results.

4. DISCISSION AND CONCLUSION

Lenard has introduced the effective cross section concept. After a great success of the Bohr's theory of the hydrogen atom, in which energies of stationary states are crucial, the energy is

used rather than velocity of incident electrons as the independent variable. During decades, beside the total, the integrated (integral, momentum transfer and viscosity) cross sections were defined (see brief review in the paper by Žigman and Milić[53]). We have been using this concept dominantly in our electron-atom scattering studies.

For inelastic scattering, Bethe[54] established another, the generalized oscillator strength (GOS) concept, with the momentum transfer as the key variable for analyzing of fast particle collisions. In the intermediate energy region, where the first Born approximation is unrealistic, continuation of the Fano plot appears for He.[55] Probably, it is not "fortuitous", because our experimental results show similar behavior of Ar, Kr and Xe resonance states[56].

In the case of argon and the rare gases, electron diffraction could be assigned as a process whit a dominant contribution to the shapes and magnitudes of differential and integrated cross sections. Though electron exchange is also possible, its effects become less important for the heavier atoms (Ar, Kr, Xe, Rn) in the energy region between 10 and 100 eV.

We analyzed positions of the minima in the case of Ar (fig. 4.1). Lower angle minima are without any structure around the critical point at 68.5° and 41.3 eV, but the position of the higher angle minimum changes in vicinity of the critical point at 143.5° and 37.3 eV[24].

Critical points, were a "collapse" of DCS appear, could be responsible for rapid decrease of integrated cross sections. At the energy region between 10 and 100 eV, there is only one critical point in the case Ne, so remarkable influence to integrated cross sections is not suspected in this case, but Ar has two critical points, so one can suspect such influence. Only one critical point of Kr, could be discussed similarly as that of Ne. There are four critical points in the case of Xe, between 10 and 100 eV, so it would be an explanation of the prominent structure in its $Q_i = Q_i(E)$ as well as $D_\lambda = D_\lambda(E)$ curves.

It is clear from figures 3.3 and 3.5 that diffraction is remarkable process, because the value of D_λ is comparable with one, for Ar, Kr, Xe and Rn, in the energy region from 10 to 100 eV. Physical meaning of D_λ is obviously the atomic size "seen" by the incident electron. The reduced effective atomic diameter changes vs. incident electron energy in such a way that prominent structure appears in the case of Ar and Xe (and perhaps Rn). It is important to note that all experiments with high energy and angular resolution confirm the structure of D_λ between 10 and 100 eV. On the contrary, only relativistic "one-channel" and "two-channel" calculations by Duisburg group (Awe *et al.*[57], Kemper *et al.*[58]) confirm the structure in Xe.

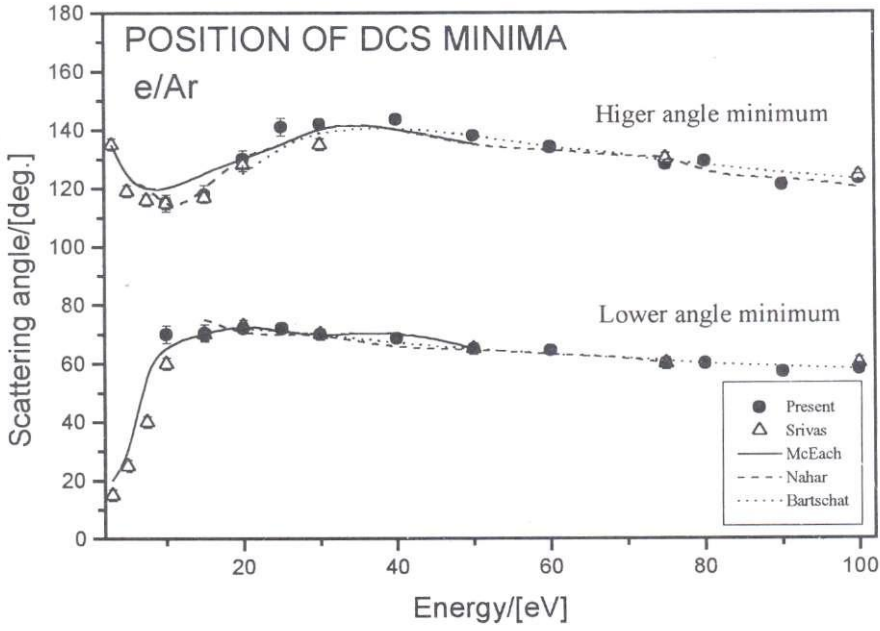

Figure 4.1. Position of DCS minima vs. incident electron energy in elastic e/Ar scattering: •, present; Δ, Srivastava *et al.*[25]; —, McEachran and Stauffer[60]; ---, Nahar and Wadehra[61]; ···, Bartschat *et al*[13].

Experimental investigation of the electron absorption effect in the case of elastic scattering of electrons by argon[59] has shown that the optical potential used in the calculation by Bartschat *et al.*[13] is probably not complete because it includes at most ten inelastic channels. Statistical weight ratios for fine structure states are also important for correct estimation of the contribution of a separate inelastic channel[29,30]. The structure reported here is an encouragement for new, more accurate electron – argon and the rare gas atom cross section measurements in the intermediate energy region. Sophisticated theoretical approaches must be improved to reproduce the structure reported here.

REFERENCES

1. P. Lenard, *Ann. d. Phys.*, **12** (1903) 714.
2. J. Franck and G. Hertz, Verh. d. D. Phys. Ges., **16** (1914) 10.
3. C. Ramsauer, *Ann. d. Phys.*, **66** (1921) 546.
4. H.F. Mayer, *Ann. d. Phys.*, **64** S (1921) 451.

5. H. Faxen und J. Holtsmark, *Z. f. Phys.* **45** (1927) 307.
6. F.L. Arnot, *Proc.Roy.Soc.* **133** (1931) 615.
7. E.C. Bullard and H.S.W. Massey, *Proc.Roy.Soc.* **130** (1931) 579.
8. M. Born, *Z. f. Phys.* **38** (1926) 803.
9. N.F. Mott and H.S.W. Massey, *The Theory of Atomic Collisions*, II ed. Oxford, 1949.
10. G.J. Schulz, *Rev.Mod.Phys.* **45** (1973) 378.
11. M.H. Mittleman and K.M. Watson, *Phys.Rev.* **113** (1959) 198.
12. H. Yoshioka, *J.Phys Soc.Japan* **12** (1957) 618.
13. K. Bartschat, R.P. McEachran and A.D. Stauffer, *J.Phys B: At.Mol.Opt.Phys.* **21** (1988) 2789.
14. B. Bederson, in *Fundamental Processes in Atomic Collision Physics*, eds. H.Kleinpoppen, J.S. Briggs and H.O. Lutz (1985), p.133.
15. I.C. Percival and M.J. Seaton, *Phyl.Trans.Roy.Soc. A* **251** (1958) 113.
16. G.E. Chamberlain, J.A. Simpson, S.R. Mielczarek and C.E. Kuyatt, *J.Chem.Phys.* **47** (1967) 4266.
17. S.G. Kukolich, *Am.J.Phys.* **36** (1968) 701.
18. R.L.J. Guunshor, *Appl. Phys.* **2** (1965) 654.
19. M.S. Dababneh, Y.F. Hcieh, W.E. Kauppila, V. Pol and T.S.Stein, *Phys. Rev. A* **26** (1982) 1252.
20. K. Jost, P.G.F. Bisling, F. Eschen, M. Felsmann and L. Walther, *13th ICPEAC*, Berlin (1983) p. 91, and private communication.
21. M. Hayashi, *J.Phys D: Appl. Phys.* **16** (1983) 581.
22. D.F. Register, S. Trajmar and S.K. Srivastava, *Phys.Rev. A* 21 (1980) 1134.
23. D.F. Register and S. Trajmar, *Phys.Rev. A* 29 (1984) 1785.
24. R. Panajotović, D. Filipović, B. Marinković, V. Pejčev, M. Kurepa and L.Vušković, *J.Phys B: At.Mol.Opt.Phys.* **30** (1997) 5877.
25. S.K. Srivastava, H. Tanaka, A. Chutjian and S. Trajmar, *Phys.Rev. A* 23 (1981) 2156.
26. D.M. Filipović, PhD Thesis, Faculty of natural sciences, University of Belgrade, Yugoslavia.
27. L.T. Sin Fai Lam, *J.Phys. B: At.Mol.Opt.Phys.* **15** (1982) 119.
28. G.A. Cook, *Argon, Helium and the Rare Gases* vol I, ed G.A. Cook (New York: Interservice, 1981) p. 1.
29. D.M. Filipović, V. Pejčev, B.P. Marinković and L. Vušković, *J.Phys. B: At.Mol.Opt.Phys.* **33** (2000) 677.
30. D.M. Filipović, B.P. Marinković, V. Pejčev and L. Vušković, *J.Phys. B: At.Mol.Opt.Phys.* **33** (2000) 2081.
31. F.J. de Heer, R.H.J. Jansen and W. van der Kaay, *J.Phys. B: At.Mol.Opt.Phys.* **12** (1979) 979.
32. R.W.Wagenaar and F.J. de Heer, *J.Phys. B: At.Mol.Opt.Phys.* **13** (1980) 3855.
33. W.E. Kauppila, T.S. Stein, J.H. Smart, M.S. Dababneh, Y.K. Ho, J.P. Downing and V. Pol, *Phys.Rev. A* **24** (1981) 725.

34. M. Hayashi, (1981) *Recommended Values of Transport Cross Sections for Elastic Collision and Total Collision Cross Section for Electrons in Atomic and Molecular Gases,* Nagoya University, Nagoya, Japan, and private communication.
35. J.C. Nickel, K. Imre, D.F.Register and S.Trajmar, *J.Phys. B: At.Mol.Opt.Phys.* **18** (1985) 125.
36. S.J. Buckman and B. Lohmann, *J.Phys. B: At.Mol.Opt.Phys.* **13** (1986) 2547.
37. H.C. Straub, P. Renault, B.G. Lindsay, K.A. Smith and R.F. Stebbings, *Phys.Rev. A* **52** (1995) 1115.
38. S.K. Srivastava, H. Tanaka, A. Chutjian and S. Trajmar, *Phys.Rev.A* **23** (1981) 2156.
39. J.F. Williams and B.A. Willis, *J.Phys. B: At.Mol.Opt.Phys.* **8** (1975) 1670.
40. R.D. DuBois and M.E Rudd, *J.Phys. B: At.Mol.Opt.Phys.* **9** (1976) 2657.
41. D.F. Register, S. Trajmar and S.K. Srivastava, *Phys.Rev.A* **21** (1980) 1134.
42. S. Kalezić, M. Kurepa, B. Predojević and D.M. Filipović, 1997, 3rd General Conference of the Balkan Physical Union, Cluj-Napoca, Romania, Book of Abstracts, p. 92.
43. F.L. Arnot, Proc.Roy.Soc. **133** (1931) 615.
44. M. Fink and A.C. Yates, Technical Report No.88, The University of Texas, Austin, 1970.
45. S.C. Gupta and J.A. Rees, *J.Phys. B: At.Mol.Opt.Phys.* **8** (1975) 417.
46. D.F. Register and S. Trajmar, *Phys.Rev.A* **29** (1984) 1785.
47. D. Andric (unpublished), in D.F. Register and S. Trajmar, *Phys.Rev.A* **29** (1984) 1785.
48. K.J. Kollath and C.B. Lucas, Z.Physik A 292 (1979) 215.
49. J. Kessler, J. Liedke and C.B. Lukas, 8th SPIG, Dubrovnik, Yugoslavia (1976) p. 61-64.
50. E. Dorn, Abh.Naturforsch.Ges.Halle/S 22 (1900) 155.
51. R.B. Randels, K.T. Chao and H.R. Crane, *Phys.Rev.* **68** (1945) 64.
52. R.T. Brinkmann and S. Trajmar, *J.Phys.E: Sci. Instrum.*, **14** (1981) 245.
53. V.J. Žigman and B.S. Milić, *J.Phys. B: At.Mol.Opt.Phys.* **21** (1988) 2609.
54. H. Bethe, *Ann.Phys.* **81** (1930) 325.
55. M. Inokuti, *Rev.Mod.Phys*. **41** (1971) 297.
56. D.M. Filipović, B. Predojević, V. Pejčev, B.P. Marinković and L. Vušković, 10th Congress of Yugoslav Physicians, Vrnjačka Banja, 2000, Book of Contributed Papers, p. 71.
57. B. Awe, F. Kemper, F. Rosicky and R.Feder, *J.Phys. B: At.Mol.Opt.Phys.* **16** (1983) 603.
58. F. Kemper, F. Rosicky and R. Feder, *J.Phys. B: At.Mol.Opt.Phys.* **18** (1985) 1223. and private communication.
59. J. Matijević, R. Panajotović, B. Marinković, V. Pejčev and D.M. Filipović, 18th SPIG, Kotor, Yugoslavia (1996) p. 40-42.
60. R.P. McEachran and A.D. Stauffer, *J.Phys. B: At.Mol.Opt.Phys.* **16** (1983) 4023.
61. S.N. Nahar and J.M. Wadehra, *Phys.Rev.A* **35** (1987) 2051.